

Stereo-topographic mapping of the Stratigraphy of Mars' South Polar Layered Deposits

P. Becerra (1), M.M. Sori (2), N. Thomas (1), A. Pommerol (1), M. Almeida (1), S. Tulyakov (3), A. Ivanov (3,4), E. Simioni (5), G. Cremonese (5), and The CaSSIS Team.

(1) Physikalisches Institut, Universität Bern, Bern, Switzerland (2) University of Arizona, Tucson, AZ, USA (3) École polytechnique fédérale de Lausanne, Lausanne, Switzerland (4) Space Center, Skolkovo Institute of Technology, Moscow, Russia (5) INAF, Osservatorio Astronomico di Padova, Padova, Italy

Abstract

We correlate exposures of SPLD beds in different locations using stereo data from MRO's HiRISE and from TGO's CaSSIS instrument.

1. Introduction

The Polar Layered Deposits (PLD) of Mars are km-thick deposits of stratified H_2O ice and dust, observable remotely because of exposures of their inner structure in scarps at their margins and spiral troughs throughout [1]. Observations of these exposures in the north PLD [2] support the theory that this stratigraphic record is influenced by climate variations forced by Mars' insolation history [3–5].

The southern deposits (SPLD; Fig. 1a), which appear to be at least an order of magnitude older than the NPLD [6,7], have exposed strata that are thicker, darker, and more eroded than in the north [8–10]. In addition, the prospect of tying a climate record to the SPLD is hindered by the solutions for Mars' past orbital evolution becoming chaotic earlier than ~20 Ma [4], younger than the estimated SPLD surface age. These problems have resulted in fewer studies of the SPLD in comparison to its northern counterpart.

Here, we map SPLD stratigraphy at high resolution using HiRISE Digital Terrain Models (DTMs; Fig. 1b) and the first stereo-images taken by TGO's CaSSIS [11], which although not able to view the southernmost latitudes, can observe the northern margin of the SPLD ($130^\circ E$ – $220^\circ E$; Fig. 1a). This region likely represents a separate stratigraphic unit, which CaSSIS will be able to extensively study in stereo; the first science phase passes have already acquired observations of bed exposures in UL (Fig. 1c). We search for dominant periodicities in the stratigraphy, and attempt to correlate exposures in different regions of the SPLD to determine if a consistent climate signal is recorded throughout [12].

2. Methods

We use data analysis methods similar to those used for the NPLD by [2]. The dataset (Fig. 1)

consists of 8 HiRISE-based DTMs [13] of bed exposures spread out across the SPLD, and approximately 12 CaSSIS stereo pairs (most are planned for the imaging cycles in the next month), at least two of which will be available for analysis by the time of the conference. At the time of writing, these methods have been applied to the HiRISE data, and will be applied to the available CaSSIS data before EPSC. As in [2], we extract local slope (at the vertical resolution of the DTMs, ~1m for HiRISE, ~8 m for CaSSIS), and bed protrusion (a property explained in [12], which is a proxy for resistance to erosion) from the DTMs. Five individual linear profiles taken ~10 m apart along strike (~ 30 m for CaSSIS) are averaged to minimize noise due to smaller-scale effects (Fig. 1c). Fig. 2 shows average protrusion profiles for each HiRISE study site.

We visually compare topographic profiles through the different SPLD sites (e.g. Fig. 2) and we use dynamic time warping (DTW) to quantitatively correlate profiles from different sites. The DTW method tunes a function to another to test for a possible high covariance between the two (here, depth is a proxy for time) and has been validated for use in Mars' PLD [14].

We search for periodicities in the continuous linear profiles using Wavelet Analysis [2]. The wavelet power spectra (WPS) reveal any dominant periodic forcing frequencies in the data, providing another tool for correlating strata from different sites and informing future investigations into the putative orbitally-forced deposition of the SPLD.

3. Results: HiRISE

Protrusion profiles for 7 of the 8 HiRISE sites are shown in Fig 2. The exposure at site S1 does not overlap in elevation range with any other site and thus is not shown. However, a lack of elevation overlap does not necessarily imply no correlation, as accumulation rates can vary widely over the PLD [2].

Results from wavelet analysis seem consistent with the general picture in Fig. 2 (example WPS for S0 are shown in Fig. 3). S3 and S6 have similar

dominant wavelengths in protrusion (22 m and 14 m) and slope. The lower 5 sites have larger dominant wavelengths in protrusion ($S_0 = 72$ m, $S_4 = 102$ m, $S_5 = 47$ m, $S_2 = 34$ m, $S_7 = 135$ m), and in slope. Additionally, DTW correlation results (not shown here) suggest a similar structure. We hypothesize that the three sets of profiles correspond to three different accumulation periods. A 3-sequence structure was suggested before by [9]. This study correlated exposures of similar units based on morphology, but a quantitative correlation is still missing.

The WPS also suggest that at least regional climate signals exist in the SPLD, but the exposure stratigraphy of the SPLD appears more complex and less consistent than that found in the NPLD. Ongoing radar analysis suggests these difficulties may also exist in beds that are not exposed at the surface [15].

4. Future Work

An expanded dataset of DTMs will significantly improve our work, as was the case for the NPLD. We have targeted numerous new areas in the SPLD for DTM creation. In particular, extensive CaSSIS coverage of Ultima Lingula (UL) - where we only have one HiRISE DTM - will help define whether UL represents an entirely different stratigraphic unit, or if it can be correlated to the Promethei Lingula Layer sequence (PLL) of [9], and will provide the most detailed stratigraphic mapping of the region to date. Additionally, there is also only one HiRISE DTM in the highest areas of the SPLD (S_1), so we have also targeted this area for HiRISE DTM production to obtain a complete picture of the accumulation history of the SPLD.

Further in the future, we plan to statistically compare the dominant wavelengths in the stratigraphy to the possible orbital scenarios before 20 Ma proposed by [4]. As was done for the north by [2], and for equatorial deposits by [16], we will compare the average ratios of wavelengths in the stratigraphic data to that of the possible oscillations of the average insolation [3].

5. Figures

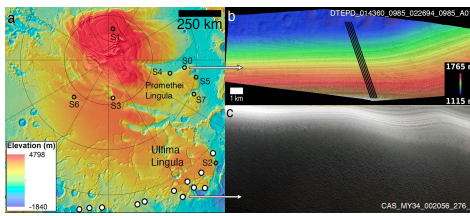


Fig. 1. (a) MOLA map of the SPLD with study sites indicated. Labeled open circles = HiRISE DTMs. White-filled circles = Planned/Executed CaSSIS Stereo. (b) HiRISE DTM of site S0 with profiles drawn (c) 1st CaSSIS color stereo pair of the UL margin. Filters: NIR-RED-PAN [11]. Location shown by arrow.

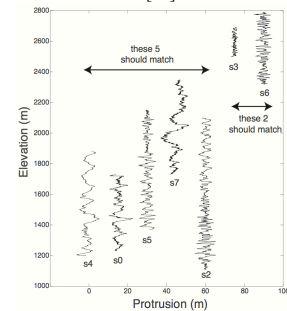


Fig. 2. Average protrusion profiles from HiRISE DTMs as a function of elevation for 7 sites in the SPLD. Profiles are offset in increments of 15 m on the x-axis for better visibility.

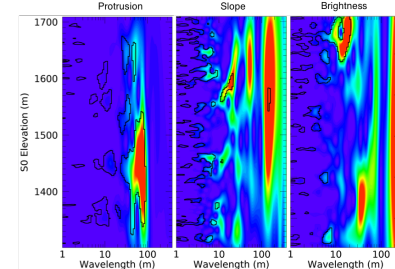


Fig. 3. Wavelet Power Spectra of the protrusion, slope, and brightness profiles of site S0. Warmer colors indicate higher power. Black lines are contours denoting the 95% confidence level over red noise (see [2] for details).

Acknowledgements

The authors wish to thank the TGO/CaSSIS spacecraft and instrument engineering teams for the successful completion of the instrument. CaSSIS is a project of the University of Bern and funded through the Swiss Space Office via ESA's PRODEX programme. The instrument hardware development was also supported by the Italian Space Agency (ASI) (ASI-INAF agreement no. I/018/12/0), INAF/Astronomical Observatory of Padova, and the Space Research Center (CBK) in Warsaw. Support from SGF (Budapest), the University of Arizona and NASA are also gratefully acknowledged. The authors also thank the HiRISE Science and Operations team for the acquisition of the images and the production of the DTMs.

References

- [1] Byrne et al. *Ann. Rev. Earth Planet. Sci.* (2009)
- [2] Becerra et al. *GRL* (2017)
- [3] Laskar et al. *Science* (2002)
- [4] Laskar et al. *Icarus* (2004)
- [5] Hvidberg et al. *Icarus* (2012)
- [6] Herkenhoff et al. *Icarus* (2000)
- [7] Koutnik et al. *JGR* (2002)
- [8] Byrne and Ivanov, *JGR* (2004)
- [9] Milkovich and Plaut, *JGR* (2008)
- [10] Limaye et al. *JGR* (2012)
- [11] Thomas et al. *Space Sci. Rev.* (2017)
- [12] Becerra et al. *JGR* (2016)
- [13] Kirk et al. *JGR* (2008)
- [14] Sori et al. *Icarus* (2014)
- [15] Whitten et al. *AGU* (2017)
- [16] Lewis et al. *Science* (2008)